HHS Public Access

Author manuscript

Exp Physiol. Author manuscript; available in PMC 2019 July 01.

Published in final edited form as:

Exp Physiol. 2018 July ; 103(7): 1020–1029. doi:10.1113/EP086988.

MITOPROTECTION PRESERVES THE RENAL VASCULATURE IN PORCINE METABOLIC SYNDROME

Alfonso Eirin, MD[1], **Ahmad F. Hedayat, MD**[1], **Christopher M. Ferguson**[1], **Stephen C. Textor, MD**[1], **Amir Lerman, MD**[2], and **Lilach O. Lerman, MD, PhD**[1,2]

[1]Division of Nephrology and Hypertension, Mayo Clinic, Rochester, MN

[2]Cardiovascular Diseases, Mayo Clinic, Rochester, MN

Abstract

Background—The metabolic syndrome (MetS) induces intra-renal microvascular disease, which may involve mitochondrial injury. The mitochondrial cardiolipin-targeting peptide elamipretide (ELAM) improves the microcirculation in post-stenotic kidneys, but its ability to attenuate MetS-induced renal vascular damage is unknown. We hypothesized that chronic treatment with ELAM would decrease renal vascular remodeling and function in swine MetS.

Methods—Pigs were studied after 16 weeks of diet-induced MetS, MetS treated for the last 4 weeks with daily injections of ELAM (0.1mg/kg), and Lean controls (n=6 each). Single-kidney regional perfusion, blood flow (RBF) and glomerular filtration rate (GFR) were measured with multi-detector-CT. Peritubular capillary (PTC) endothelial cell (EC) mitochondrial density and cardiolipin content were assessed in situ, as were PTC-EC apoptosis and oxidative stress. The spatial density of PTC (H&E staining) and renal microvessels (micro-CT), and renal artery endothelial function (organ bath) were characterized.

Results—Regional perfusion and serum creatinine were preserved in MetS pigs, but RBF and GFR were higher compared to Lean. Mitochondrial density and cardiolipin content were diminished in MetS PTC-EC, but improved in ELAM-treated pigs, as did PTC density. ELAM also attenuated PTC-EC oxidative stress and apoptosis. Furthermore, ELAM improved renal microvascular density, decreased microvascular remodeling, and restored endothelial nitric oxide (eNOS) expression and endothelial-dependent relaxation of renal artery segments.

Conclusions—MetS-induced mitochondrial alterations might contribute to renal PTC and microvascular loss, and impair renal artery endothelial function in pigs. Mitoprotection with

Correspondence: Lilach O. Lerman, MD, PhD, Division of Nephrology and Hypertension, Mayo Clinic, 200 First Street SW, Rochester, MN, 55905. Lerman.Lilach@Mayo.Edu Phone: (507)-266-9376, Fax: (507)-266-9316.

Competing interests

None declared.

Author contributions

A.E. and L.O.L. conceived and designed the study. A.E. A.F.H. and C.M.F. performed the experiments, analyzed the data and prepared the figures. A.E., S.C.T., A.L., and L.O.L: drafted the manuscript. All authors approved the final version of the manuscript and agree to be accountable for all aspects of the work in ensuring that questions related to the accuracy or integrity of any part of the work are appropriately investigated and resolved. All persons designated as authors qualify for authorship, and all those who qualify for authorship are listed.

ELAM preserved a hierarchy of renal vessels, underscoring its potential to ameliorate renal vascular injury in MetS.

Keywords

Metabolic syndrome; Mitochondria; Kidney; Cardiolipin; Microvascular

INTRODUCTION

The metabolic syndrome (MetS) is defined as a constellation of major cardiovascular risk factors, including obesity, hypertension, dyslipidemia, and insulin resistance, that reflect over-nutrition and sedentary lifestyles. The prevalence of the MetS is increasing to epidemic proportions (Cameron *et al.*, 2004), increasing a person's risk of cardiovascular disease, stroke, and all-cause mortality (Martins *et al.*, 2010; Ferraro *et al.*, 2011). MetS has also been associated with the development and progression of chronic kidney disease (CKD) (Thomas *et al.*, 2011), partly because diabetes and hypertension remain the primary causes of CKD and end-stage renal disease (ESRD) (Saran *et al.*, 2017).

The renal circulation is a structural and functional network composed by large vessels (e.g. renal arteries) that progressively branch into medium-side and small microvessels, glomerular capillaries, and finally peritubular capillaries (PTCs) that surround renal tubules to ensure tissue perfusion and remove unwanted substances from the filtrate (Chade & Hall, 2016). We have previously shown that MetS in Ossabaw pigs is associated with renal microvascular remodeling and immaturity (Li *et al.*, 2011a). We have also shown that the number of cortical microvessels and PTC density were diminished in domestic pigs with diet-induced MetS, indicating microvascular loss (Eirin *et al.*, 2018). Importantly, microvascular remodeling and loss are known contributors to the progression of renal injury (Anderson *et al.*, 2009). However, the exact mechanisms of MetS-induced renal vascular damage remain to be fully elucidated.

Unlike tubular cells that are rich in mitochondria, mitochondrial content in endothelial cells (ECs) is relatively modest (Caja & Enriquez, 2017). Nevertheless, these mitochondria may be important because renal ECs regulate vascular function, partly by modulating cell death, oxidative stress, and nitric oxide (NO) bioavailability (Kluge *et al.*, 2013). For example, increased oxidative stress in renal EC mitochondria induces p53, promoting translocation of the pro-apoptotic Bax (Cheng *et al.*, 2007), and generation of mitochondrial reactive oxygen species (ROS) inhibits antiapoptotic factors, such as B-cell lymphoma 2 (BCL-2), leading to apoptosis (Green & Reed, 1998). Furthermore, excess of mitochondrial ROS activates cellular NADPH oxidase and the subsequent formation of superoxide. These in turn interacts with NO, forming peroxinitrate, which damages the respiratory complexes I and III, diminishing NO bioavailability and creating a vicious cycle of oxidative stress, mitochondrial injury, and endothelial dysfunction (Doughan *et al.*, 2008). Therefore, treatment strategies that preserve the morphology and function of EC mitochondria may ameliorate MetS-induced renal vascular damage.

Mitochondrial-targeted peptides are small compounds that specifically target mitochondrial pathways. Elamipretide (ELAM) is a small synthetic tetrapeptide that concentrates in the

mitochondrion, specifically binding and stabilizing cardiolipin, an essential constituent of the inner mitochondrial membrane implicated in the formation of cristae membranes and energy production (Szeto, 2014b). Cardiolipin possesses a unique conical shape that favors the formation of cristae in the inner membrane (Szeto, 2014a), and interacts with inner membrane proteins, contributing to the formation of supercomplexes that enhance energy production. Cardiolipin also interacts with cytochrome-c, potentiating its role as an electron carrier, and its preservation with ELAM prevents cytochrome-c peroxidase activity, ameliorating oxidative stress (Birk *et al.*, 2014). ELAM also prevents formation of the mitochondrial permeability transition pore, and the subsequent release of cytochrome-c to the cytosol to initiate apoptosis. Importantly, mitochondrial uptake of ELAM is independent of membrane potential, as opposed to some other mitochondria-targeted antioxidants (e.g. mito-tempo, mito-Q, etc.) (Zhao *et al.*, 2004). Therefore, ELAM potentiates electron transport chain activity and exerts important antioxidant and antiapoptotic effects that can protect ECs. We have previously shown in swine with renal artery stenosis that treatment with ELAM preserved the renal microcirculation in the post-stenotic kidney (Eirin *et al.*, 2012b; Eirin *et al.*, 2014), but whether this approach preserves the renal vasculature in MetS has not been explored. Therefore, this study tested the hypothesis that chronic treatment with ELAM would decrease renal vascular remodeling and function in swine MetS.

METHODS

Ethical Approval

All animal experiments were performed with the approval of the Institutional Animal Care and Use Committee (#A3291-01) and conform to the principles and regulations, as described in the Principles and standards for reporting animal experiments (Grundy, 2015).

Animal characteristics and experimental protocol

Eighteen 3-month old female domestic pigs (Manthei Hog Farm, Elk River, MN) were studied after 16 weeks of observation. At baseline 12 animals started a high-cholesterol/carbohydrate diet (MetS) (Pawar *et al.*, 2015), and the remaining 6 animals a standard pig chow (Lean).

After 12 weeks of diet, 6 MetS pigs started treatment with daily subcutaneous injections of ELAM (Stealth BioTherapeutics, Inc., Newton, MA), 0.1mg/kg in 1mL of phosphate-buffered saline (PBS), 5 days/week for the following 4 weeks, whereas a PBS vehicle was injected in the remaining 6 MetS pigs.

Four weeks later, pigs were anesthetized with 0.25 g of IM tiletamine hydrochloride/zolazepam hydrochloride and 0.5 g of xylazine, and maintained with IV ketamine (0.2 mg/kg/minute) and xylazine (0.03 mg/kg/minute). Single-kidney hemodynamics and function were assessed using multi-detector computed tomography (MDCT), and mean arterial pressure using an arterial catheter inserted in the left carotid artery, as previously described (Krier *et al.*, 2001).

Fasting blood samples were collected before MDCT studies to assess plasma renin activity (PRA), and levels of creatinine (Eirin *et al.*, 2011a), total cholesterol, low-density lipoprotein

(LDL), triglyceride levels, as well as glucose and insulin levels for calculation of the homeostasis model assessment of insulin resistance (HOMA-IR) (Li *et al.*, 2011b; Zhang *et al.*, 2013; Pawar *et al.*, 2015).

One week later, animals were euthanized with a lethal bolus of 100mg/kg of sodium pentobarbital in the ear vein (Khangura *et al.*, 2014). The kidneys were removed using a retroperitoneal incision and immediately dissected. A segment of the kidney was prepared for micro-CT studies, and the remaining kidney tissue frozen in liquid nitrogen or preserved in formalin or Trump's fixative for ex-vivo studies. Distal branches of the renal artery were dissected and placed in Krebs solution for in vitro endothelial function studies.

In-vivo studies—MDCT scanning was performed using a 128 scanner (128-Slice Somatom Definition Flash, Siemens Medical Solution, Forchheim, Germany), an ultra-fast scanner that provides noninvasive quantifications of single-kidney regional perfusion and renal blood flow (RBF) (Krier *et al.*, 2001; Eirin *et al.*, 2012a). In brief, an iopamidol bolus (0.5 ml/kg per 2 seconds) was injected two seconds after initiation of scanning. Image acquisition consisted of 70 scans that cycled every 0.57 seconds, followed by 70 scans with a 2 second cycle, resulting in 140 sequential images collected over 3 minutes (Daghini *et al.*, 2007b) with intermittent assisted ventilation. Blood pressure was monitored throughout the experiment. Three adjacent 5-mm slices were collected at each time point and reconstructed using a D30f kernel. Endothelium-dependent microvascular reactivity was tested by repeating the same flow study after a 10-min intra-aortic infusion of acetylcholine (Ach, 5mg/kg/min). In addition, kidneys were scanned from pole to pole in the continuous volume scanning mode (6mm section thickness) during a short central venous infusion of iopamidol (0.5ml/kg per 5 seconds) to sustain corticomedullary differentiation (vascular phase) throughout volume scanning (Daghini *et al.*, 2007a). Cross-sectional MDCT images were reconstructed, analyzed using Analyze™ (Biomedical Imaging Resource, Mayo Clinic, MN), and renal cortical and medullary perfusion and RBF were calculated, as previously described (Krier *et al.*, 2001; Eirin *et al.*, 2012a). Briefly, regions of interest were selected from the aorta, renal cortex, and medulla (Figure 1) and tissue time-attenuation curves were analyzed using a modified γ-variable model (Daghini *et al.*, 2007b) that yielded curve-fitting algorithms to measure cortical and medullary perfusion. Cortical and medullary volumes were calculated using the planimetry method, whereas RBF computed as the sum of the products of cortical and medullary perfusions and volumes, and GFR calculated from the cortical proximal-tubular curve (Daghini *et al.*, 2007a).

Ex-vivo studies

PTC EC mitochondrial morphology and cardiolipin content

Mitochondrial density and morphology was assessed in randomly selected PTC-ECs (5 per pig, a total of 30 per group), using a digital electron microscopy (Philips CM10). The number of mitochondria/cell was averaged to obtain mitochondrial number, and mitochondrial area and matrix density measured using Image-J software (Parra *et al.*, 2014; Szeto *et al.*, 2015). PTC-EC cardiolipin content and PTC localization were assessed by double immunofluorescence staining with 10N-nonyl acridine-orange (A1372; Invitrogen, Carlsbad, CA) and the PTC endothelial marker plasmalemma vesicle-associated protein

(pLVAP, NBP2-19868; Novus Biologicals, Littleton, CO), respectively. Images were quantified in 15–20 random fields using a computer-aided image analysis program (ZEN®2012 blue edition, Carl ZEISS SMT, Oberkochen, Germany). The number of PTCs was quantified in a blinded fashion in sections stained with Hematoxylin and Eosin (H&E), as previously described (Eirin *et al.*, 2012b).

PTC EC apoptosis and oxidative stress

PTC-EC apoptosis was assessed in kidney sections double-stained with pLVAP and terminal deoxynucleotidyl transferase-mediated dUTP nick-end labeling (TUNEL; Promega, Madison, WI). The number of pLVAP/TUNEL+ cells was quantified and averaged in each group. PTC-EC oxidative stress was assessed by double immunofluorescence staining of pLVAP with nitrotyrosine, and quantified using ZEN®. All quantifications were performed in a blinded manner.

Renal microvascular architecture

Under physiological pressure, one kidney from each pig was perfused with a radio-opaque silicone polymer (Microfil MV122, Flow Tech, Carver, MA), using a saline-filled cannula (PE 190) and a syringe infusion pump (SIP 22; Harvard Apparatus, Holliston, MA) until the polymer drained freely from a segmental vein. Perfused sections were preserved in 10% buffered formalin, and then scanned using a micro-CT scanner, which generates 3D images consisting of up to a billion cubic voxels, each 5μm to 25μm on a side, with isotropic spatial resolution. Images were reconstructed (20μm voxels), and spatial density of cortical and medullary microvessels (diameters 20–500μm) calculated using Analyze™, as previously described (Zhu *et al.*, 2004; Favreau *et al.*, 2010). Vessel tortuosity was assessed by the "connectivity index" (vessel length divided by the shortest distance between its ends) (Bentley *et al.*, 2002). In addition, media-to-lumen ratio was calculated in randomly selected intra-renal vessels in α smooth muscle actin (SMA)-stained sections (DakoCytomation A/S, Glostrup, Denmark).

Renal inflammation and fibrosis

Before MDCT scans and under fluoroscopic guidance, catheters were advanced into the renal vein and blood samples collected, centrifuged, and plasma aliquots stored at −80°C. Renal vein levels of interleukin (IL)-1β, tumor necrosis factor (TNF)-α, and IL-6 were measured by luminex (Millipore, Billerica, MA) (Yuan *et al.*, 2018). Additionally, renal fibrosis was assessed in renal cross-sections staining with trichrome, which was semi-automatically quantified in 15–20 fields in a blinded manner.

Renal vascular endothelial function

Dissected renal artery sections (2–3mm long, one per animal) were suspended in 25ml organ chambers (one per renal artery ring) filled with Kreb's solution at 37°C (pH=7.4, 95% O_2, and 5% CO_2). Isometric force was measured by suspending the renal artery sections using 2 stainless clips passed through their lumen attached to a stationary post and a strain gauge. Vessels were then allowed to equilibrate for 30 minutes after washing with control solution. Following precontraction with endothelin-1 (10^{-7}M, Phoenix Pharmaceuticals, Mountain

View, CA), increasing concentrations of acetylcholine (Ach, 10^{-9}–10^{-4}M) were added to the bath to evaluate endothelium-dependent relaxation, or endothelium-independent-vasodilation with sodium nitroprusside (SNP, 10^{-9}–10^{-4}M). Data was quantified using WinDaq Acquisition Software (DATAQ Instruments, Inc. Akron, OH).

In addition, cardiolipin staining, eNOS expression, and apoptosis (TUNEL) were assessed in these renal artery sections, as was production of superoxide anion by dihydroethidium (DHE) staining.

Statistical analysis

All data were analyzed using JMP Pro 13 (SAS Institute Inc., Cary, NC). The Shapiro-Wilk test was used to assess the distribution normality of the tested variables. Normally distributed variables were expressed as mean±standard deviation and compared with One-way analysis of variance (ANOVA) and unpaired t-test with Tukey's post hoc. For data that did not show a Gaussian distribution, results were expressed as median (range) and comparisons within and among the groups performed using non-parametric tests (Wilcoxon and Kruskal Wallis, respectively) with Steel-Dawss post hoc. All tests were two-tailed, and p-values ≤0.05 were considered statistically significant.

For comparison purposes, renal hemodynamics and function, as well as in-vitro renal vascular endothelial function, were assessed in 6 matched Lean animals that were treated with daily injections of ELAM (0.1mg/kg).

RESULTS

After 16 weeks of diet, body weight was higher in MetS and MetS+ELAM compared to Lean pigs (91.8±2.1kg and 91.3±4.5kg vs. 72.3±11.1kg, respectively, both $p<0.05$) and lipid fractions were higher in both MetS groups (Table 1). Fasting insulin levels were also higher in MetS and MetS+ELAM compared to Lean (0.7±0.05μU/ml and 0.7±0.05μU/ml vs. 0.4±0.09μU/ml, respectively, both $p<0.05$), as were HOMA-IR levels (1.8±0.15 and 1.7±0.34 vs. 0.6±0.07, respectively, both $p<0.05$). Contrarily, fasting glucose were similar among Lean, MetS, and MetS+ELAM (129.8±36.5mg/dl, 117.2±18.1mg/dl, and 116.7±32.7mg/dl, respectively, all, $p>0.05$), as were PRA, serum creatinine, and cortical and medullary perfusion (Table 1). Renal volume was similarly elevated in MetS and MetS +ELAM compared to Lean, whereas cortical and medullary perfusion did not differ among the groups. Basal RBF and GFR were similarly elevated in MetS and MetS+ELAM compared to Lean, whereas a significant increase in RBF in response to Ach was similar among the groups.

ELAM preserves PTC EC mitochondria

Electron microscopy revealed that the number of PTC-EC mitochondria was markedly lower in MetS compared to Lean, but normalized in MetS+ELAM (Figure 2A). Although PTC-EC mitochondrial area did not differ among the groups, matrix density that decreased in MetS, improved in ELAM-treated pigs. Similarly, EC cardiolipin content decreased in MetS compared to Lean, but was fully restored to normal levels in MetS+ELAM (Figure 2B).

Mitoprotection attenuates PTC-EC damage

The number of capillaries per tubule decreased in MetS compared to Lean, but improved in MetS+ELAM (Figure 2C). The number of pLVAP/TUNEL apoptotic and pLVAP/nitrotyrosine-positive cells was higher in the MetS compared to Lean, but normalized in ELAM-treated pigs (Figure 3).

ELAM ameliorates MetS-induced renal microvascular remodeling

Spatial density of cortical microvessels substantially decreased in MetS, but improved in ELAM-treated pigs (Figure 4A). Furthermore, medullary microvascular density that decreased in MetS normalized in MetS+ELAM. Vessel tortuosity, which reflects vascular immaturity, was greater in MetS compared to Lean, but restored to normal levels in ELAM-treated pigs (Figure 4B). Vessel wall-to-lumen ratio, which was higher in MetS versus to Lean, also decreased in MetS+ELAM (Figure 4C).

ELAM attenuates renal inflammation

Renal vein levels of IL-1β and TNF-α were higher in MetS groups compared to Lean, but decreased in ELAM-treated pigs (Figure S1A), whereas elevated renal vein levels of IL-6 remained unaltered in MetS+ELAM. Tubulointerstitial fibrosis did not differ among the groups (Figure S1B).

ELAM improves renal artery endothelial function

The vasorelaxation response to Ach in excised renal artery rings was impaired in MetS compared to Lean, but normalized in MetS+ELAM, whereas the response to SNP was unchanged (Figure S2A). Cardiolipin content in renal artery sections was decreased in MetS, but restored in MetS-ELAM, as did eNOS immunoreactivity (Figure S2B). The number of apoptotic cells (TUNEL) in renal artery rings increased in MetS, but decreased in MetS +ELAM, associated with decreased production of superoxide anion (DHE).

ELAM does not affect renal function in Lean animals

Blood pressure, lipid fractions, serum creatinine, PRA, as were as renal volume, cortical and medullary perfusion, GFR, and RBF, and its response to Ach did not differ between Lean and Lean+ELAM (Table 1). In addition, the vasorelaxation response to Ach and SNP in excised renal artery rings was similar in Lean and Lean+ELAM (Figure S2A), as were cardiolipin and eNOS expression, apoptosis, and production of superoxide anion (Figure S2B).

DISCUSSION

The present study shows that experimental MetS exerts important changes in small, medium, and large renal vessels, including decreased PTC and microvascular density, microvascular remodeling (tortuosity and thickening), and impaired endothelial-dependent relaxation of renal artery segments. Furthermore, the number and matrix density of PTC-EC mitochondria was markedly lower in MetS compared to Lean pigs, suggesting mitochondria injury in endothelial cells. Notably, preservation of mitochondrial cardiolipin improved PTC-EC

mitochondrial density and attenuated apoptosis and oxidative stress, which were associated with protection of the renal microvasculature and restoration of renal artery endothelial function. These findings underscore the direct contribution of mitochondrial injury to the pathogenesis of MetS-induced vascular damage, and reveal a unique potential of ELAM for preserving the vasculature in experimental MetS.

The prevalence of MetS has been on the rise over the last couple of decades, increasing the risk of CKD and ESRD (Ferraro *et al.*, 2011). Previous studies have shown that MetS damages the renal circulation. For example, obesity in mice is associated enhanced vascular contractility to angiotensin-II (Barton *et al.*, 2000) and increased responsiveness to vasoconstrictor peptides (Baretella *et al.*, 2014). In line with this, we have previously shown that a diet-induced MetS in Ossabaw swine is associated with intrarenal and perirenal adiposity, and microvascular tortuosity, suggesting formation of immature microvessels (Li *et al.*, 2011a). Furthermore, MetS diet in domestic pigs decreases cortical microvascular and PTC density, reflecting microvascular loss (Eirin *et al.*, 2018). Importantly, dysfunctional or damaged vessels can progressively impair renal perfusion, filtration, and tubular function (Chade, 2013), underscoring the need to design novel therapies to protect the renal vasculature in patients with MetS.

The current study extends our previous observations in renovascular disease (Eirin *et al.*, 2012b; Eirin *et al.*, 2014), demonstrating that daily treatment with ELAM for 4 weeks preserves a hierarchy of renal vessels in swine MetS. Particularly, ELAM improved the number of PTCs, which are among the most vulnerable renal structures in the face of acute or chronic insults. PTCs are critical for delivering oxygen and nutrients to tubular epithelial cells and play an important role in mediating reabsorption and secretion processes between the blood and glomerular filtrate. Indeed, the extent of PTC rarefaction predicts interstitial damage and renal functional decline in patients with CKD (Kida *et al.*, 2014). In the current study, improvement of the number of PTCs by ELAM was associated with restoration of EC cardiolipin content, mitochondrial number, and matrix density, underscoring the role of mitochondria in regulating the PTC circulation in experimental MetS.

Capillary rarefaction results from interplay among several pathogenic mechanisms, including apoptosis, oxidative stress, and reduced availability of vasoactive substances. PTC-ECs undergoing apoptosis have increased pro-coagulant and pro-adhesive properties, contributing to capillary occlusion, thrombosis, and inflammation, ultimately exacerbating PTC loss (Winn & Harlan, 2005). Oxidative stress-induced PTC-EC obliteration reduces PTC flow, inducing tubular ischemic injury and tubulointerstitial fibrosis (Futrakul *et al.*, 2002). Interestingly, this study shows that treatment with ELAM attenuated PTC-EC oxidative stress and apoptosis, possibly by preventing release of pro-oxidant and pro-apoptotic factors to the cytosol. Therefore, these observations support a direct effect of mitochondrial protection to ameliorate MetS-induced PTC EC apoptosis and oxidative stress.

ELAM also improved larger renal microvessels, a network of medium size cortical and medullary vessels that envelops each nephron. We and others have shown that microvascular remodeling and loss correlate with progressive deterioration of renal perfusion and tubular

function, and are important determinants of renal dysfunction (Iliescu *et al.*, 2010; Eirin *et al.*, 2011b). In this study, we found that loss of cortical and medullary microvessels was substantially improved in MetS+ELAM pigs, resembling our previous observations in renovascular disease (Eirin *et al.*, 2012b; Eirin *et al.*, 2014). Similarly, ELAM attenuated microvascular remodeling, reflected by the decrease in vessel tortuosity and media-to-lumen ratio, uncovering its potential to preserve the renal microvasculature in MetS.

Preservation of intra-renal PTCs and microvessels in ELAM-treated pigs was also accompanied by improvements in endothelial-dependent relaxation of renal artery segments in vitro, denoted by responses to Ach, likely due to restoration of cardiolipin and eNOS immunoreactivity. Improved endothelial function may be attributed to mitoprotection that reduced apoptosis and oxidative stress, disclosed by decreased TUNEL positive cells and DHE staining. Contrarily, RBF response to Ach, reflecting endothelium-dependent microvascular reactivity in small vessels, was significant in all groups compared to baseline, suggesting that MetS-induced endothelial dysfunction is more pronounced in large vessels. Importantly, protection of renal artery segments and those at the level of the renal microcirculation and PTCs may result in preservation of tissue perfusion, glomerular filtration, and tubular function in the late stages of MetS.

Notably, treatment with ELAM attenuated renal inflammation, disclosed by reduced renal vein levels of the pro-inflammatory cytokines IL-1β and TNF-α. Increased generation of inflammatory cytokines from the renal parenchyma and adipose tissues contributes to renal microvascular damage, favoring progression of chronic kidney injury in obesity (Chade & Hall, 2016). Therefore, MetS-induced renal inflammation, in conjunction with renal oxidative stress and apoptosis, may have partly accounted for renal microvascular remodeling and tortuosity in our model.

Despite significant improvements in the renal vasculature, ELAM did not affect blood pressure, likely due to recruitment of non-renal pressor mechanisms in MetS (Garovic & Textor, 2005). Alternatively, it is not unlikely that residual minor renal damage combined with systemic dyslipidemia fostered unrelenting hypertension. Furthermore, RBF and GFR remained similarly higher in MetS and MetS+ELAM compared to Lean, possibly due to their higher body weight. Thus, MetS-induced increments in RBF and intra-vascular volume might have masked the impact of ELAM on preservation of cortical and medullary microvessels.

Importantly, renal hemodynamics and function were similar between Lean and Lean +ELAM, as were renal artery cardiolipin and eNOS expression, apoptosis, production of superoxide anion, and endothelial function, underscoring our previous observations (Eirin *et al.*, 2014; Eirin *et al.*, 2015) that ELAM does not affect renal structure and function, and redox status in healthy subjects.

The limitations of this study included the short duration of the diet, the lack of a Vehicle-treated Lean group, and the use of relatively young animals. Furthermore, our model does not allow discrimination among the role of obesity, hypertension, hyperlipidemia, and insulin reistance in the pathogenesis of MetS-induced renal vascular injury. However, this

disease cluster, and renal structure and function in our swine model, are analogous to those in patients, and thus represent many renal aspects of clinical MetS. Nevertheless, further studies are needed to define the individual effect of each componnent of MetS on renal vascular damage and its reversibility by mitoprotection.

In summary, our study shows that mitoprotection with ELAM preserved mitochondrial density and cardiolipin content, and improved both the structure and function of the renal circulation. At the level of capillaries, ELAM increased the number of PTC-ECs, and attenuated their oxidative stress and apoptosis. In larger renal microvessels ELAM attenuated remodeling and loss, while in renal artery segments it improved endothelial-dependent relaxation. Therefore, our observations are consistent with the notion that MetS-induced mitochondrial alterations might impair small, medium, and large renal vessels, and suggest a potential role for mitoprotection in ameliorating renal vascular injury in MetS. Further studies are needed to determine the long-term effect of ELAM and to establish its vasculoprotective properties in patients with MetS.

Acknowledgments

Funding

This work was supported by a research grant from Stealth Biotherapeutics, Inc., and from the NIH (DK106427, DK104273, HL123160, and DK102325).

References

Anderson S, Halter JB, Hazzard WR, Himmelfarb J, Horne FM, Kaysen GA, Kusek JW, Nayfield SG, Schmader K, Tian Y, Ashworth JR, Clayton CP, Parker RP, Tarver ED, Woolard NF, High KP. workshop p. Prediction, progression, and outcomes of chronic kidney disease in older adults. J Am Soc Nephrol. 2009; 20:1199–1209. [PubMed: 19470680]

Baretella O, Chung SK, Barton M, Xu A, Vanhoutte PM. Obesity and heterozygous endothelial overexpression of prepro-endothelin-1 modulate responsiveness of mouse main and segmental renal arteries to vasoconstrictor agents. Life Sci. 2014; 118:206–212. [PubMed: 24412387]

Barton M, Carmona R, Morawietz H, d'Uscio LV, Goettsch W, Hillen H, Haudenschild CC, Krieger JE, Munter K, Lattmann T, Luscher TF, Shaw S. Obesity is associated with tissue-specific activation of renal angiotensin-converting enzyme in vivo: evidence for a regulatory role of endothelin. Hypertension. 2000; 35:329–336. [PubMed: 10642320]

Bentley MD, Rodriguez-Porcel M, Lerman A, Sarafov MH, Romero JC, Pelaez LI, Grande JP, Ritman EL, Lerman LO. Enhanced renal cortical vascularization in experimental hypercholesterolemia. Kidney Int. 2002; 61:1056–1063. [PubMed: 11849461]

Birk AV, Chao WM, Bracken C, Warren JD, Szeto HH. Targeting mitochondrial cardiolipin and the cytochrome c/cardiolipin complex to promote electron transport and optimize mitochondrial ATP synthesis. Br J Pharmacol. 2014; 171:2017–2028. [PubMed: 24134698]

Caja S, Enriquez JA. Mitochondria in endothelial cells: Sensors and integrators of environmental cues. Redox Biology. 2017; 12:821–827. [PubMed: 28448943]

Cameron AJ, Shaw JE, Zimmet PZ. The metabolic syndrome: prevalence in worldwide populations. Endocrinology and Metabolism Clinics of North America. 2004; 33:351–375. [PubMed: 15158523]

Chade AR. Renal vascular structure and rarefaction. Compr Physiol. 2013; 3:817–831. [PubMed: 23720331]

Chade AR, Hall JE. Role of the Renal Microcirculation in Progression of Chronic Kidney Injury in Obesity. Am J Nephrol. 2016; 44:354–367. [PubMed: 27771702]

Cheng J, Cui R, Chen CH, Du J. Oxidized low-density lipoprotein stimulates p53-dependent activation of proapoptotic Bax leading to apoptosis of differentiated endothelial progenitor cells. Endocrinology. 2007; 148:2085–2094. [PubMed: 17289842]

Daghini E, Juillard L, Haas JA, Krier JD, Romero JC, Lerman LO. Comparison of mathematic models for assessment of glomerular filtration rate with electron-beam CT in pigs. Radiology. 2007a; 242:417–424. [PubMed: 17255413]

Daghini E, Primak AN, Chade AR, Krier JD, Zhu XY, Ritman EL, McCollough CH, Lerman LO. Assessment of renal hemodynamics and function in pigs with 64-section multidetector CT: comparison with electron-beam CT. Radiology. 2007b; 243:405–412. [PubMed: 17456868]

Doughan AK, Harrison DG, Dikalov SI. Molecular mechanisms of angiotensin II-mediated mitochondrial dysfunction: linking mitochondrial oxidative damage and vascular endothelial dysfunction. Circ Res. 2008; 102:488–496. [PubMed: 18096818]

Eirin A, Ebrahimi B, Zhang X, Zhu XY, Tang H, Crane JA, Lerman A, Textor SC, Lerman LO. Changes in glomerular filtration rate after renal revascularization correlate with microvascular hemodynamics and inflammation in Swine renal artery stenosis. Circ Cardiovasc Interv. 2012a; 5:720–728. [PubMed: 23048054]

Eirin A, Ebrahimi B, Zhang X, Zhu XY, Woollard JR, He Q, Textor SC, Lerman A, Lerman LO. Mitochondrial protection restores renal function in swine atherosclerotic renovascular disease. Cardiovasc Res. 2014; 103:461–472. [PubMed: 24947415]

Eirin A, Lerman A, Lerman LO. Mitochondria: a pathogenic paradigm in hypertensive renal disease. Hypertension. 2015; 65:264–270. [PubMed: 25403611]

Eirin A, Li Z, Zhang X, Krier JD, Woollard JR, Zhu XY, Tang H, Herrmann SM, Lerman A, Textor SC, Lerman LO. A mitochondrial permeability transition pore inhibitor improves renal outcomes after revascularization in experimental atherosclerotic renal artery stenosis. Hypertension. 2012b; 60:1242–1249. [PubMed: 23045468]

Eirin A, Zhu XY, Jonnada S, Lerman A, Van Wijnen AJ, Lerman LO. Mesenchymal stem cell-derived extracelular vesicles improve the renal microvasculature in metabolic renovascular disease in swine. Cell Transplant. 2018 In Press.

Eirin A, Zhu XY, Urbieta-Caceres VH, Grande JP, Lerman A, Textor SC, Lerman LO. Persistent kidney dysfunction in swine renal artery stenosis correlates with outer cortical microvascular remodeling. Am J Physiol Renal Physiol. 2011a; 300:F1394–1401. [PubMed: 21367913]

Eirin A, Zhu XY, Urbieta-Caceres VH, Grande JP, Lerman A, Textor SC, Lerman LO. Persistent kidney dysfunction in swine renal artery stenosis correlates with outer cortical microvascular remodeling. Am J Physiol Renal Physiol. 2011b; 300:F1394–1401. [PubMed: 21367913]

Favreau F, Zhu XY, Krier JD, Lin J, Warner L, Textor SC, Lerman LO. Revascularization of swine renal artery stenosis improves renal function but not the changes in vascular structure. Kidney Int. 2010; 78:1110–1118. [PubMed: 20463652]

Ferraro PM, Lupo A, Yabarek T, Graziani MS, Bonfante L, Abaterusso C, Gambaro G. Incipe Study G. Metabolic syndrome, cardiovascular disease, and risk for chronic kidney disease in an Italian cohort: analysis of the INCIPE study. Metab Syndr Relat Disord. 2011; 9:381–388. [PubMed: 21711121]

Futrakul N, Tosukhowong P, Valyapongpichit Y, Tipprukmas N, Futrakul P, Patumraj S. Oxidative stress and hemodynamic maladjustment in chronic renal disease: a therapeutic implication. Ren Fail. 2002; 24:433–445. [PubMed: 12212823]

Garovic VD, Textor SC. Renovascular hypertension and ischemic nephropathy. Circulation. 2005; 112:1362–1374. [PubMed: 16129817]

Green DR, Reed JC. Mitochondria and apoptosis. Science. 1998; 281:1309–1312. [PubMed: 9721092]

Grundy D. Principles and standards for reporting animal experiments in The Journal of Physiology and Experimental Physiology. J Physiol. 2015; 593:2547–2549. [PubMed: 26095019]

Iliescu R, Fernandez SR, Kelsen S, Maric C, Chade AR. Role of renal microcirculation in experimental renovascular disease. Nephrol Dial Transplant. 2010; 25:1079–1087. [PubMed: 19934087]

Khangura KK, Eirin A, Kane GC, Misra S, Textor SC, Lerman A, Lerman LO. Cardiac function in renovascular hypertensive patients with and without renal dysfunction. Am J Hypertens. 2014; 27:445–453. [PubMed: 24162729]

Kida Y, Tchao BN, Yamaguchi I. Peritubular capillary rarefaction: a new therapeutic target in chronic kidney disease. Pediatr Nephrol. 2014; 29:333–342. [PubMed: 23475077]

Kluge MA, Fetterman JL, Vita JA. Mitochondria and endothelial function. Circ Res. 2013; 112:1171–1188. [PubMed: 23580773]

Krier JD, Ritman EL, Bajzer Z, Romero JC, Lerman A, Lerman LO. Noninvasive measurement of concurrent single-kidney perfusion, glomerular filtration, and tubular function. Am J Physiol Renal Physiol. 2001; 281:F630–638. [PubMed: 11553509]

Li Z, Woollard JR, Wang S, Korsmo MJ, Ebrahimi B, Grande JP, Textor SC, Lerman A, Lerman LO. Increased glomerular filtration rate in early metabolic syndrome is associated with renal adiposity and microvascular proliferation. Am J Physiol Renal Physiol. 2011a; 301:F1078–1087. [PubMed: 21775485]

Li Z, Woollard JR, Wang S, Korsmo MJ, Ebrahimi B, Grande JP, Textor SC, Lerman A, Lerman LO. Increased glomerular filtration rate in early metabolic syndrome is associated with renal adiposity and microvascular proliferation. Am J Physiol Renal Physiol. 2011b; 301:F1078–1087. [PubMed: 21775485]

Martins D, Ani C, Pan D, Ogunyemi O, Norris K. Renal dysfunction, metabolic syndrome and cardiovascular disease mortality. J Nutr Metab. 2010

Parra V, Verdejo HE, Iglewski M, Del Campo A, Troncoso R, Jones D, Zhu Y, Kuzmicic J, Pennanen C, Lopez-Crisosto C, Jana F, Ferreira J, Noguera E, Chiong M, Bernlohr DA, Klip A, Hill JA, Rothermel BA, Abel ED, Zorzano A, Lavandero S. Insulin stimulates mitochondrial fusion and function in cardiomyocytes via the Akt-mTOR-NFkappaB-Opa-1 signaling pathway. Diabetes. 2014; 63:75–88. [PubMed: 24009260]

Pawar AS, Zhu XY, Eirin A, Tang H, Jordan KL, Woollard JR, Lerman A, Lerman LO. Adipose tissue remodeling in a novel domestic porcine model of diet-induced obesity. Obesity (Silver Spring). 2015; 23:399–407. [PubMed: 25627626]

Saran R, Robinson B, Abbott KC, Agodoa LY, Albertus P, Ayanian J, Balkrishnan R, Bragg-Gresham J, Cao J, Chen JL, Cope E, Dharmarajan S, Dietrich X, Eckard A, Eggers PW, Gaber C, Gillen D, Gipson D, Gu H, Hailpern SM, Hall YN, Han Y, He K, Hebert H, Helmuth M, Herman W, Heung M, Hutton D, Jacobsen SJ, Ji N, Jin Y, Kalantar-Zadeh K, Kapke A, Katz R, Kovesdy CP, Kurtz V, Lavalee D, Li Y, Lu Y, McCullough K, Molnar MZ, Montez-Rath M, Morgenstern H, Mu Q, Mukhopadhyay P, Nallamothu B, Nguyen DV, Norris KC, O'Hare AM, Obi Y, Pearson J, Pisoni R, Plattner B, Port FK, Potukuchi P, Rao P, Ratkowiak K, Ravel V, Ray D, Rhee CM, Schaubel DE, Selewski DT, Shaw S, Shi J, Shieu M, Sim JJ, Song P, Soohoo M, Steffick D, Streja E, Tamura MK, Tentori F, Tilea A, Tong L, Turf M, Wang D, Wang M, Woodside K, Wyncott A, Xin X, Zang W, Zepel L, Zhang S, Zho H, Hirth RA, Shahinian V. US Renal Data System 2016 Annual Data Report: Epidemiology of Kidney Disease in the United States. Am J Kidney Dis. 2017; 69:A7–A8. [PubMed: 28236831]

Szeto HH. First-in-class cardiolipin-protective compound as a therapeutic agent to restore mitochondrial bioenergetics. Br J Pharmacol. 2014a; 171:2029–2050. [PubMed: 24117165]

Szeto HH. First-in-class cardiolipin-protective compound as a therapeutic agent to restore mitochondrial bioenergetics. British Journal of Pharmacology. 2014b; 171:2029–2050. [PubMed: 24117165]

Szeto HH, Liu S, Soong Y, Birk AV. Improving mitochondrial bioenergetics under ischemic conditions increases warm ischemia tolerance in the kidney. Am J Physiol Renal Physiol. 2015; 308:F11–21. [PubMed: 25339695]

Thomas G, Sehgal AR, Kashyap SR, Srinivas TR, Kirwan JP, Navaneethan SD. Metabolic syndrome and kidney disease: a systematic review and meta-analysis. Clin J Am Soc Nephrol. 2011; 6:2364–2373. [PubMed: 21852664]

Winn RK, Harlan JM. The role of endothelial cell apoptosis in inflammatory and immune diseases. J Thromb Haemost. 2005; 3:1815–1824. [PubMed: 16102048]

Yuan F, Hedayat AF, Ferguson CM, Lerman A, Lerman LO, Eirin A. Mitoprotection attenuates myocardial vascular impairment in porcine metabolic syndrome. Am J Physiol Heart Circ Physiol. 2018; 314:H669–H680. [PubMed: 29196345]

Zhang X, Li ZL, Woollard JR, Eirin A, Ebrahimi B, Crane JA, Zhu XY, Pawar AS, Krier JD, Jordan KL, Tang H, Textor SC, Lerman A, Lerman LO. Obesity-metabolic derangement preserves hemodynamics but promotes intrarenal adiposity and macrophage infiltration in swine renovascular disease. Am J Physiol Renal Physiol. 2013; 305:F265–276. [PubMed: 23657852]

Zhao K, Zhao GM, Wu D, Soong Y, Birk AV, Schiller PW, Szeto HH. Cell-permeable peptide antioxidants targeted to inner mitochondrial membrane inhibit mitochondrial swelling, oxidative cell death, and reperfusion injury. J Biol Chem. 2004; 279:34682–34690. [PubMed: 15178689]

Zhu XY, Chade AR, Rodriguez-Porcel M, Bentley MD, Ritman EL, Lerman A, Lerman LO. Cortical microvascular remodeling in the stenotic kidney: role of increased oxidative stress. Arterioscler Thromb Vasc Biol. 2004; 24:1854–1859. [PubMed: 15308558]

New Findings

What is the central question of this study?

We hypothesized that chronic mitoprotection would decrease renal vascular remodeling and dysfunction in swine metabolic syndrome.

What is the main finding and its importance?

This study shows that experimental metabolic syndrome exerts renal microvascular and endothelial cell mitochondrial injury, which were attenuated by mitoprotection, underscoring the contribution of mitochondrial injury to the pathogenesis of metabolic syndrome-induced vascular damage.

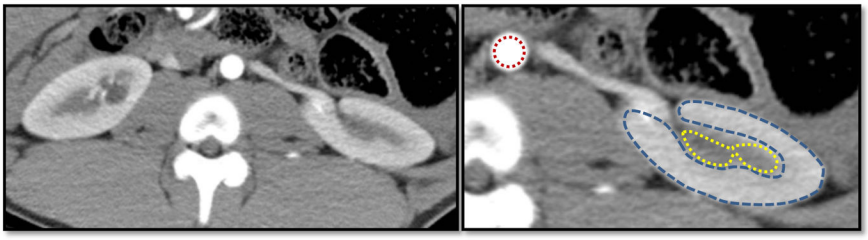

Figure 1.
Representative cross-sectional MDCT image of the kidney showing aortic (red), as well as cortical (blue) and medullary (yellow) regions of interest.

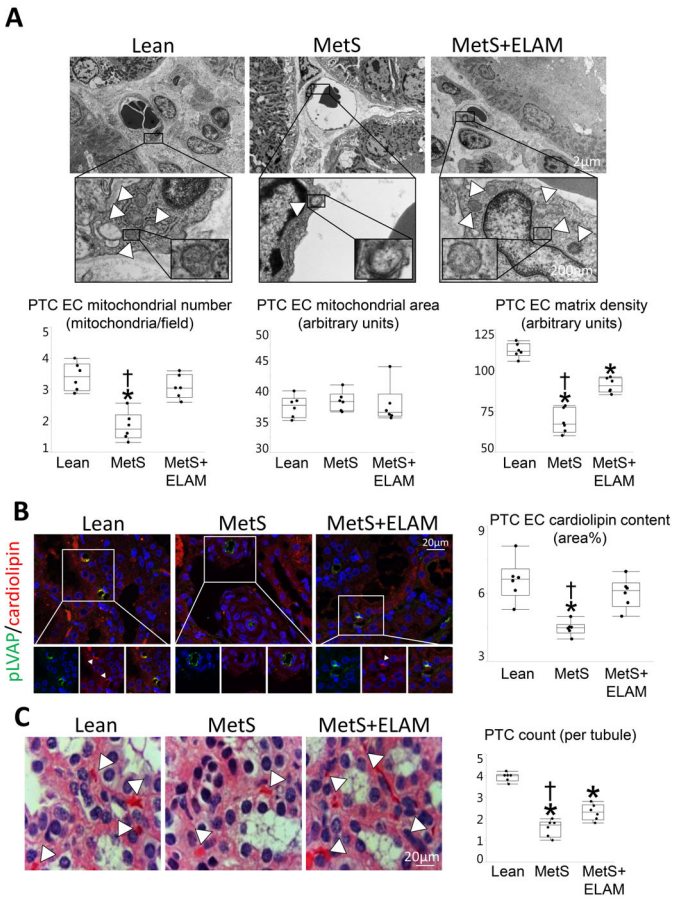

Figure 2. ELAM attenuates endothelial cell (EC) mitochondrial injury and restores cardiolipin content

A: Transmission electron microscopy and quantification of PTC-EC mitochondrial number and area, and matrix density (5 PTC-ECs per animal, 6 animals/group). B: Representative double immunofluorescent staining (40X) for the PTC-EC marker plasmalemma vesicle associated protein (pLVAP, green) and the mitochondrial inner membrane phospholipid cardiolipin (red) showing decreased endothelial mitochondria and cardiolipin expression (merge yellow) in MetS, which was normalized in ELAM-treated pigs (n=6/group). C: Representative H&E-stained kidney sections (x40 images). The number of capillaries per tubule decreased in MetS compared to Lean, but improved in MetS+ELAM (n=6/group). *p<0.05 vs. Lean, †p<0.05 vs. MetS+ELAM.

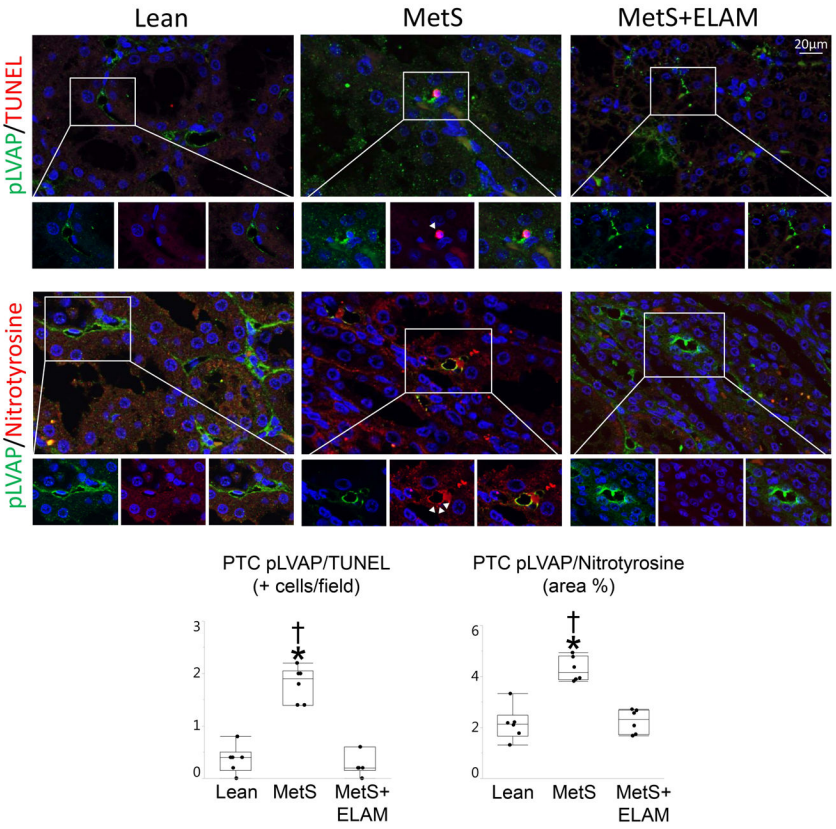

Figure 3.

ELAM ameliorates peritubular capillary (PTC) endothelial cell (EC) injury. Representative double immunofluorescent staining (40X) for pLVAP (green) and terminal deoxynucleotidyl transferase-mediated dUTP nick end labeling (TUNEL), nitrotyrosine, and eNOS (red). The number of PTC EC (pLVAP, green) positive for TUNEL (red) was elevated in MetS, but decreased to normal levels in MetS+ELAM (n=6/group). Treatment with ELAM restored double-immunoreactivity of nitrotyrosine (red) and pLVAP (n=6/group). *p<0.05 vs. Lean, †p<0.05 vs. MetS+ELAM.

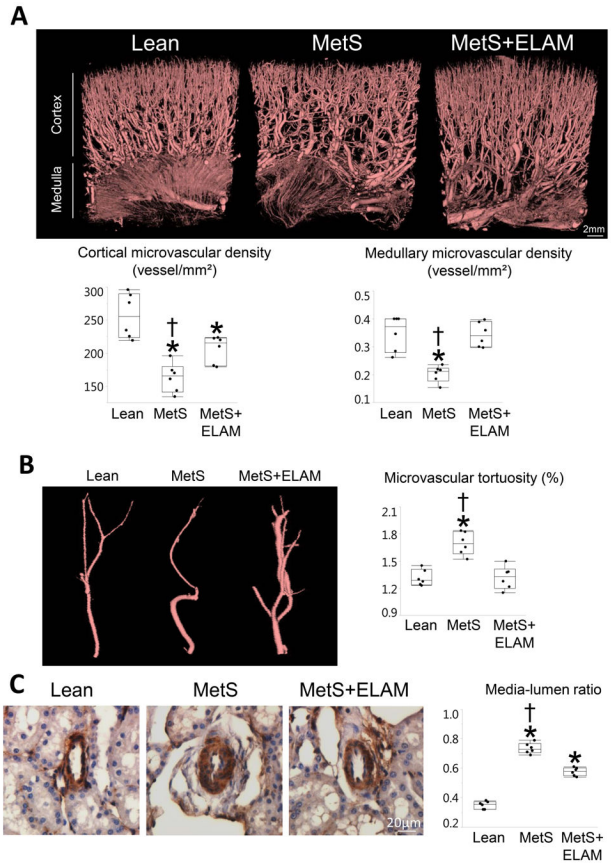

Figure 4. ELAM improved PTC and microvascular remodeling

A: Representative 3-dimensional microcomputed-tomography images of the kidney and quantification of spatial density of cortical and medullary microvessels (n=6/group). B, Vessel tortuosity was higher in MetS, but normalized in ELAM-treated pigs (n=6/group). C: Renal vessel wall-to-lumen ratio in α-smooth muscle actin (SMA) stained slides. Vessel wall-to-lumen ratio, which was higher in MetS compared to Lean, improved in ELAM-treated pigs (n=6/group). *p<0.05 vs. Lean, †p<0.05 vs. MetS+ELAM.

Table 1

Systemic characteristics and kidney hemodynamics and function in Lean, Lean+ELAM, MetS, and MetS+ELAM pigs (n=6 per group) at 16 weeks.

Parameter	Lean	Lean+ELAM	MetS	MetS+ELAM
Mean blood pressure (mmHg)	100.4±10.8	98.4±9.3	126.6±7.7 *	124.6±7.7 *
Total cholesterol (mg/dl)	82.5 (76.0–90.5)	82.4 (74.2–93.7)	414.0 (331.0–506.8) *	383.5 (306.8–410.3) *
LDL cholesterol (mg/dl)	33.8 (26.4–40.3)	36.1 (28.2–39.3)	369.7 (213.4–489.6) *	286.4 (262.6–468.1) *
Triglycerides (mg/dl)	7.4±1.7	7.4±1.5	17.9±7.8 *	16.1±5.8 *
Plasma renin activity (ng/ml/h)	0.17±0.11	0.15±0.11	0.16±0.07	0.14±0.08
Serum creatinine (mg/dl)	1.7±0.2	1.6±0.4	1.6±0.2	1.8±0.3
Renal volume (ml/min)	137.6±18.5	145.5±8.9	223.0±21.3 *	236.4±25.5 *
Cortical perfusion (ml/min/cc)	3.9±0.8	3.8±0.6	4.1±0.5	4.0±0.8
Medullary perfusion (ml/min/cc)	3.4 (2.0–3.6)	3.5 (2.6–3.9)	1.9 (3.2–1.9)	2.2 (1.8–4.1)
RBF (ml/min)	503.3±25.9	642.9±54.2	867.5±86.9 *	917.9±59.7 *
RBF response to Ach (% change)	19.1±6.8‡	16.8±10.5‡	21.8±7.5‡	16.9±5.6‡
GFR (ml/min)	79.9 (65.6–86.5)	81.0 (65.1–89.7)	154.8 (127.8–162.2) *	130.4 (128.2–140.7) *

* p≤0.05 vs. Lean,

‡ p<0.05 vs. baseline.

MetS: metabolic syndrome, ELAM: Elamipretide, LDL: Low-density lipoprotein, HOMA-IR: Homeostasis model assessment of insulin resistance, RBF: Renal blood flow, Ach: Acetylcholine, GFR: Glomerular filtration rate.